

LRP 578/97

August 1997

SILICON OXIDE PARTICLE FORMATION IN RF PLASMAS
INVESTIGATED BY INFRARED ABSORPTION
SPECTROSCOPY AND MASS SPECTROMETRY

Ch. Hollenstein, A.A. Howling, C. Courteille,
D. Magni, S. Scholz Odermatt, G.M.W. Kroesen,
N. Simons, W. de Zeeuw, W. Schwarzenbach

submitted for publication to
Journal of Physics D: Applied Physics

Silicon Oxide Particle Formation in RF Plasmas Investigated by Infrared Absorption Spectroscopy and Mass Spectrometry

Ch. Hollenstein^{a)}, A. A. Howling^{a)}, C. Courteille^{a)}, D. Magni^{a)}, S. Scholz Odermatt^{b)}, G. M. W. Kroesen^{c)}, N. Simons^{c)}, W. de Zeeuw^{c)}, W. Schwarzenbach^{d)}

a) Centre de Recherches en Physique des Plasmas, Ecole Polytechnique Fédérale de Lausanne, PPB - Ecublens, CH - 1015 Lausanne, Switzerland.

b) Laboratoire de Technologie des Poudres, Ecole Polytechnique Fédérale de Lausanne, MX - D - Ecublens, CH - 1015 Lausanne, Switzerland.

c) Eindhoven University of Technology, 5600 MB Eindhoven, The Netherlands.

d) Laboratoire de Spectrométrie Physique, Université Joseph Fourier-Grenoble 1, 140 Avenue de la Physique, BP 87, F - 38402 Saint Martin d'Herès Cedex, France.

PACS Number : 5225; 5225R; 5270; 5275; 5280.

Abstract

In situ Fourier transform infrared absorption spectroscopy has been used to study the composition of particles formed and suspended in radio-frequency discharges of silane-oxygen-argon gas mixtures. The silane gas consumption was observed by infrared absorption. The stoichiometry of the produced particles depends on the silane flow rate and was compared with commercial colloidal silica. A small proportion of silane gas produces nanometric stoichiometric particles whereas a large proportion produces larger under-stoichiometric particles. Absorption spectroscopy was sufficiently sensitive to reveal particles too small to be visually observed by laser light scattering. Post-oxidation of hydrogenated silicon particles trapped in an argon plasma by adding oxygen was demonstrated. Mass spectrometry of negative and positive ions showed an extensive range of ionic clusters which may be at the origin of particle formation. A model based on an iterative reaction sequence gives a good agreement with the measured positive ion mass spectrum.

1. Introduction

Silicon dioxide thin film deposition is widely used in semiconductor device technology. It has been intensively studied over the last thirty years, with a considerable effort to model the fundamental oxidation processes [1-4]. Experimental oxidation studies are usually performed on films, but only a few investigations on oxidized silicon particles [5-7] are reported. Otherwise, the existence of particles in the plasma is generally ignored although they may play an important rôle in the composition and quality of deposited silicon oxide.

In the first part of this paper we demonstrate the *in situ* monitoring of nanometer sized oxidised silicon particles by infrared absorption spectroscopy measurements of powder suspended in a RF plasma. The composition of SiO_x particles produced in different argon-silane-oxygen plasmas will be discussed. Powder grown in argon-silane plasma and then trapped in a pure argon discharge can be post-oxidised by admixture of oxygen to this argon plasma. Many theoretical [8,9] and experimental studies [10-12] have shown the possible rôle of plasma species such as negative ions in the oxidation process: The second part of this paper discusses the composition of the initial SiO_x ionic clusters produced in a silane-oxygen plasma as measured by mass spectrometry.

2. Experimental arrangement

The experiment was performed in a rf capacitively-coupled plasma at 13.56 MHz with 130 mm diameter electrodes. The distance between the stainless steel electrodes is 26 mm. The gas inlet, for argon and silane, is positioned at the reactor wall behind a diffusor plate minimising the influence on the powder dynamics by gas drag. To avoid reaction of silane with oxygen in the gas line, the oxygen was injected directly into the reactor through a calibrated needle valve located at the top of the reactor. All the experiments were carried out with a rf power of 10 W and a

pressure of 0.20 mbar controlled by a throttle valve. The reactor was kept at room temperature, which tends to favor powder production in silane plasmas [13]. Light scattering of a He-Ne laser beam was used to visualize the powder produced in the plasma. Visual observation was through the window perpendicular to the laser beam path (figure 1). The reactor is described in more detail in reference [14].

For the *in situ* infrared absorption measurements, ZnSe windows were mounted on diametrically opposite flanges. The spectra were measured using a Bruker IFS-66 spectrometer with a glow bar source and an external detector. The parallel beam leaving the spectrometer is directed through the plasma (single pass) and is focused by an off-axis parabolic gold mirror onto a liquid nitrogen cooled mercury-cadmium-telluride (MCT) detector (Graseby type FTIR-W24). The Fourier transform of the detector signal yields the spectrum in the 600-4500 cm^{-1} range with a chosen spectral resolution of 1 cm^{-1} . To obtain a reasonable signal to noise ratio, the measurements were performed by averaging over one hundred spectra. The minimum absorption which could be detected by the system was of the order of 0.1 % of the source intensity. Reference spectra with the plasma off were acquired before and after each measurement to check for possible influence of deposition on the windows, and for variations in the source intensity or the detector sensitivity.

For the mass spectrometer measurements, a Balzers Plasma Process Monitor type PPM 421 was used to detect neutral radicals and ions (positive and negative) with a mass range up to 2000 amu. The probe head was positioned adjacent to the electrode gap at 10 mm from the plasma boundary. The extraction orifice used for these experiments was 100 μm diameter.

3. FTIR measurements

Two types of *in situ* oxidation experiments will be described:

- i) Oxidised silicon powder production in argon-silane-oxygen plasmas;
- ii) Post-oxidation of silicon powder trapped in an argon plasma.

i) Oxidised silicon powder was produced in diluted argon-silane-oxygen discharges. In order to investigate the influence of the gas mixture on the powder composition, the silane gas flow was altered while keeping the oxygen flow unchanged. Constant total flow was maintained by adjusting the argon flow. The infrared absorption measurements were performed in steady state conditions of the powder production as monitored by laser light scattering. Figure 2 show the infrared transmitted signal, in a range of 2000-2300 cm^{-1} , through the gas and the plasma using two different silane : oxygen : argon flow rates. The spectra show the typical absorption spectrum of silane (2050-2300 cm^{-1}). The difference in the IR spectra demonstrates the influence of the silane : oxygen ratio through the silane gas consumed in the process. With decreasing silane : oxygen ratio the obvious silane absorption finishes in complete depletion of the silane gas in the discharge at a flow ratio of 0.4. A small amount of silane can be totally consumed by the oxygen.

Figures 3a and 3b show the measured absorbance spectra, from 600 to 1400 cm^{-1} , using the two previous silane to oxygen flow rates ratios corresponding to the figure 2. With high silane flow (figure 3a), powder was visually observed using the He-Ne laser light scattering system (particle size $> \lambda/10 \sim 70$ nm) while at low silane flow (figure 3b), no powder could be observed in the discharge. However, from the presence of broad features in the infrared absorption spectrum of figure 3b, it must be concluded that powder was nevertheless present in the plasma, but with particulate size below the detection limit (~ 70 nm) of the He-Ne laser scattering system used. The absorption spectroscopy technique is therefore sufficiently sensitive to reveal particles too small to be visually observed using laser light scattering. Large differences are observed between these absorption spectra: Referring to table 1 (for a non-exhaustive list of possible mode assignments), different peaks in figure 3a originating from Si-H vibrations (peaks A, C) and from Si-O excitation (peaks B, D, E) are present whereas in figure 3b, only Si-O features appear (peaks E, F). From table 1 the large peak centered near 1085 cm^{-1} in figure 3b seems to reveal the presence of stoichiometric (SiO_2) powder whereas in figure 3a the broad peak (E) indicates an under-stoichiometric powder composition. The negative peaks between 900 and 950 cm^{-1} are silane depletion gas features. For comparison the absorption spectrum of a commercial colloidal silica (Ludox LS) is shown in figure 3c. This SiO_2 , size calibrated powder

is characterized by a specific surface of 200 m²/g as measured by gas absorption (BET method, Micrometrics) and by a particle diameter of 10 nm according to dynamic light diffusion (Malvern Zetasizer 4). For this specific powder, the infrared spectrum was obtained using a Nicolet 510 FTIR spectrometer in transmission with a KBr lozenge used as mechanical support for the SiO₂ powder. As summarised in table 1, Hu *et al.* [15] attribute the peak G at 1230 cm⁻¹ to the longitudinal optical (LO) phonon mode of SiO₂, which is normally infrared inactive, but can become active for platelet particles smaller than $\lambda / 2\pi n$ (where λ and n are the wavelength of the incident radiation and the refractive index of the imbedding matrix, respectively). According to Hu *et al.* [15] the (LO) mode become active for particles smaller than 360 nm. This can explain why the G peak is present in the nanoscale Ludox powder spectra and in the plasma conditions of low silane flowrate but not in figure 3a where visible particulates are probably larger than the threshold limit of diameter. The similarity between the commercial SiO₂ powder and the plasma-produced powder (figure 3b) demonstrates that nanoscale stoichiometric silica particles can be produced within a plasma. To summarize, the composition of the resulting particle is therefore influenced by the silane to oxygen flow ratio; under-stoichiometric powder (figure 2a) was produced in a plasma containing a significant amount of undissociated silane whereas stoichiometric nanoparticulates were produced in a silane-depleted plasma (figure 2c).

ii) For the post-oxidation experiments, hydrogenated silicon powder was initially produced in a 4 % silane-in-argon (48 sccm of argon and 2 sccm of silane) discharge. After reaching steady state of the hydrogenated silicon powder production, as monitored by laser scattering, the silane gas feed was stopped, resulting in trapping of some powder in the remaining pure argon plasma. Finally, oxygen with a typical flowrate of 7.7 sccm was added to this plasma. Figure 4 represents the steady state absorbance signals, in the 600-2000 cm⁻¹ range, of powder trapped in the pure argon plasma before (figure 4a) and after (figure 4b) addition of oxygen.

The spectrum for the powder trapped in the argon plasma (figure 4a) shows three distinct peaks. Despite the different possible attributions for the absorption peaks in the range of 600-900 cm⁻¹ (see table 1), all of them lead to the conclusion that the powder produced was only composed of amorphous hydrogenated silicon. No Si-O related vibrations were found in this

trapped powder, in contrast to the results of Kroesen *et al.* [5], where oxidation features were seen in infrared absorption spectra of powder produced under similar conditions; the oxidation of the powder found in their experiment was probably due to a leak or to oxygen originating from water from the reactor chamber. The continuous increase of the absorbance signal for wavenumbers above 1400 cm^{-1} , in figure 4a, originates from Rayleigh scattering of the infrared beam by the particles suspended in the plasma.

The absorbance signal of the previously trapped powder is considerably changed when oxygen is added to the argon plasma (figure 4b). The original peaks are replaced by a broad peak between $950\text{-}1250\text{ cm}^{-1}$, which can be entirely attributed to the oxidation of the hydrogenated silicon powders. However, in contrast to figure 4a, no significant scattering contribution is found since figure 4b shows a flat absorbance signal in the range above 1400 cm^{-1} . Two possible ways are proposed to explain the loss of scattering signal caused by the addition of the small amount of oxygen: First, powder detrapping due to additional gas drag, and secondly, powder detrapping due to changes in the plasma potential topography caused by modifications in the plasma composition [16]. An oxidation post-treatment of trapped hydrogenated silicon powder by oxygen addition to an argon plasma is thereby demonstrated, but further experiments will be necessary to determine if it was a SiO_x coating of an a-Si:H core or if it was a complete oxidation.

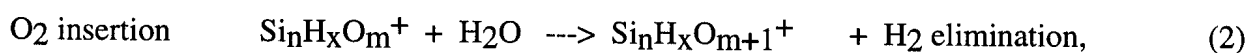
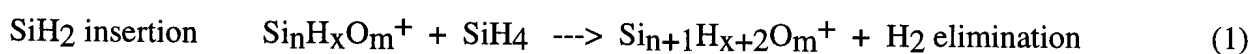
4. Mass spectrometry measurements

In addition to infrared absorption spectroscopy, mass spectrometry has been used to investigate the plasma composition during nanometer sized particle production in pure and oxygen-diluted silane plasmas. The Balzers PPM 421 plasma monitor allows the determination of neutral, positive and negative ions up to 2000 amu. In these experiments the grounded electrode was heated to 200°C and a gas mixture of 10% oxygen in silane at a total pressure of 0.1 mbar was used.

To overcome the trapping of the negative ions in the rf discharge, a power modulation technique was employed to measure the negative ion component of the plasma [17]. The plasma on-time (110 μ s) and off-time (\sim 300 μ s) gave the optimal negative ion signal. For comparison, negative and positive ion and neutral spectra of a pure silane and a diluted silane/oxygen plasma at degraded mass resolution are compared in figure 5. In both cases, very high mass anions above 1000 amu can be observed. However for both plasma conditions only lower mass cations and neutral radicals are detected. The spectrum of the diluted oxygen / silane plasma shows $\text{Si}_x\text{H}_y\text{O}_z^+$ clusters up to a similar mass limit as observed in reactions studies [18] performed by Fourier Transform mass spectrometry. Figure 6 compares the negative ion spectra at high mass resolution in pure silane and in a silane/oxygen plasmas for two different mass ranges. In figure 6a only the groups Si_nH_x^- ($n=1, 2, 3$) are presented whereas in figure 6b, intermediate groups ascribed to Si-H-O bonding appear. For higher masses (figures 6c and 6d), the rich variety of Si-O-H radical chemistry completely changes the regular structured spectrum of pure silane plasmas. In the diluted plasma each single atomic mass unit is represented in silane / oxygen plasmas from 100 amu up to at least 1000 amu. The presence of certain masses with higher abundance in the mass range between 400-600 amu might indicate clusters with particular stability. On the other hand, the regular structure of the cation spectrum (figure 5e) seems to show no special "magic number" effect as do anions and cations in pure silane.

Recently Hollenstein *et al.* [19] have shown that a statistical model for hydrogen distribution within the anionic clusters can reproduce the regular form of the measured negative ion spectra in pure silane plasmas. In diluted silane / oxygen plasmas, statistical reactions also appear to be important but to some extent, chemical structure effects will have to be included to understand the more intense peaks in the negative ion spectrum. Mandich *et al.* [18] have proposed that H_2O addition promotes positive ion clustering in silane plasmas. Following Mandich's observations, we adapted a simple model based on six empirical rules:

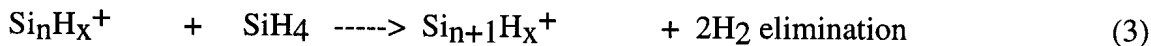
First of all we consider the following reactions (1) and (2) as being the most probable:



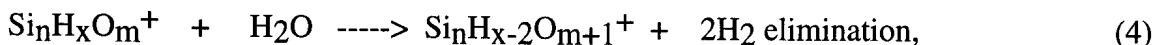
reactions (1) and (2) being the insertion of (SiH₂) 30 amu and (O) 16 amu respectively and corresponding to the energetically-favorable elimination of H₂.

Then by considering the reactions (3) and (4) as possible:

Si insertion followed by 2H₂ elimination



and O insertion followed by 2H₂ elimination as well:



reactions (3) and (4) being the addition of 28 amu and 14 amu respectively.

The fifth rule, as a consequence of the first four, forbids any reactions with atomic H elimination and so a sequence of 'odd' masses develops independently of an 'even' mass sequence. An imposed sixth rule allows only alternate addition of Si and O to the clusters and so imposes concentration equality [Si]=[O], i.e. SiO_x with x=1 for initial stoichiometry.

With the assumption that (1) and (3) are the only significant cluster growth reactions for pure silane plasmas, we introduce *f* as the branching ratio for the 'probable reaction' (1), and hence(1-*f*) is the branching ratio for the 'possible reaction' (3). Therefore, for *n* successive reactions of type (1), *n* Si atoms and (2*fn*) H atoms are added and the ratio [H]:[Si] is 2*fn* :*n* = 2*f*. According to previous measurements [19] in pure silane plasmas, the experimentally-observed [H]:[Si] ratio is 4/3 and therefore the branching ratios of the assumed reactions (1) and (3) for H₂ and 2H₂ elimination are *f* = 2/3 and 1-*f* = 1/3 respectively. Similar branching ratios for reactions (2) and (4) are arbitrarily supposed. Iteration of the reaction sequences (1) to (4) with these branching probabilities, starting from the measured abundances of the Si₂H_xO₂⁺ group, gives the calculated positive ion spectrum presented in figure 7a in which the relative isotopic abundances of silicon and oxygen have also been taken into account. A comparison between this model and high mass resolution measurements of the positive ion spectrum is presented in figure 7a and 7b for a representative part of the total mass spectrum. The overall features are clearly reproduced by the model. The reasonable agreement obtained lends some support to the assumed iterative reaction sequence scheme which is essentially a statistical model for cluster growth. Judging by the complexity of the negative ion spectrum for

silane/oxygen plasmas (figures 5d and 6d), additional reaction mechanisms must also be involved.

5. Conclusions

In situ FTIR and mass spectrometer measurements were used to investigate silane/oxygen reaction products in rf plasma. As far as the gas phase is concerned, the transmission FTIR signals have illustrated that a small proportion of silane can be totally depleted by the oxygen. As far as the created particulates are concerned, a modification in the particle chemistry with dilution could be seen; a high silane flow being able to produce large non-stoichiometric particles SiO_x , whereas a small silane flow appears to produce nano-scale stoichiometric particles quite similar to the nanometric SiO_2 commercial powder. A post-treatment oxidation of hydrogenated silicon particles was obtained by addition of oxygen to the argon plasma with a-Si:H particles trapped in it. A rich variety of Si-O-H ionic reactions was demonstrated also by means of mass spectrometry measurements. A statistical reaction scheme for the positive initial cluster growth appears to be in reasonable good agreement with the experimental results.

Acknowledgements

The authors thank M. Komer from Balzers AG for the help in mass spectrometry. This work was funded by Swiss Federal Research Grants BBW 93.0136 (for Brite-Euram project BE-7328) and BEW 9400051.

References

- [1] Landsberger L M and Tiller W A 1990 *J. Electrochem. Soc.* **137** 2825
- [2] Giunta C J, Chapple-Sokol J D and Gordon R G 1990 *J. Electrochem. Soc.* **137** 3237
- [3] Verdi L, Miotello A and Kelly R 1994 *Thin Solid Films* **241** 383
- [4] Calleja W, Falcony C, Torres A, Aceves M and Osorio R 1995 *Thin Solid Films* **270** 114
- [5] Kroesen G M W, den Boer J H W G, Boufendi L, Vivet F, Kouhli M, Bouchoule A and de Hoog F J 1996 *J. Vac. Sci. Technol. A* **14** 546
- [6] Baraton M-I 1995 *NanoStructured Materials* **5** 179
- [7] Shen T D, Koch C C, McCormick T L, Nemanich R J, Huang J Y and Huang J G 1995 *L. Mater. Res.* **10** 139
- [8] Taylor S, Eccleston W and Barlow K J 1988 *J. Appl. Phys.* **64** 6515
- [9] Taylor S, Zhang J F and Eccleston W 1993 *Semicond. Sci. Technol.* **8** 1426
- [10] O'Hanlon J F and Pennebaker W B 1971 *Appl. Phys. Lett.* **18** 554
- [11] Moruzzi J L, Kiermasz A and Eccleston W 1982 *Plasma Physics* **24** 605
- [12] Hu Y Z, Joseph J and Irene E A 1991 *Appl. Phys. Lett* **59** 1353
- [13] Dorier J-L, Hollenstein Ch and Howling A A 1995 *J. Vac. Sci. Technol. A* **13** 918
- [14] Courteille C, Hollenstein Ch, Dorier J-L, Gay P, Schwarzenbach W, Howling A A, Bertran E, Viera G, Martins R and Macarico A 1996 *J. Appl. Phys.* **80** 2069
- [15] Hu S M 1980 *J. Appl. Phys.* **51** 5945
- [16] Dorier J-L, Hollenstein Ch, Howling A A, Courteille C, Schwarzenbach W, Merad A and Boeuf J-P 1995 Special Issue : Images in Plasma Science, *IEEE Trans. Plasma Sci.* **24** 101
- [17] Howling A A, Sansonnens L, Dorier J-L and Hollenstein Ch 1994 *J. Appl. Phys.* **75** 1340
- [18] Mandich M L and Reents W D 1992 *J. Chem. Phys.* **96** 4233

- [19] Hollenstein Ch, Schwarzenbach W, Howling A A, Courteille C, Dorier J-L and Sansonnens L 1996 *J. Vac. Sci. Technol. A* **14** 535
- [20] Brodsky M H, Cardona M and Cuomo J J 1977 *Phys. Rev. B* **16** 3556
- [21] Shanks H, Fang C J, Ley L, Cardona M, Demond F J and Kalbitzer S 1980 *Phys. Stat. Sol.* **100** 43
- [22] Yacobi B G, Collins R W, Moddel G, Viktorovitch P and Paul W 1981 *Phys. Rev. B* **24** 5907
- [23] Lucovsky G, Yang J, Chao S S, Tyler J E and Czubytyj W 1983 *Phys. Rev. B* **28** 3225
- [24] Lucovsky G and Pollard W B 1983 *Physica* **117B&118B** 865
- [25] Hiraki A *Amorphous Semiconductor Technologies & Devices* (North-Holland Publishing Co. 1984)
- [26] Lucovsky G, Chao S S, Yang J, Tyler J E and Czubytyj W 1984 *J. Vac. Sci. Technol. A* **2** 353
- [27] EMIS and d. series, *Properties of Amorphous Silicon* (INSPEC, The Institution of Electrical Engineers, London, 1989).
- [28] Cicala G, Capezzuto P and Bruno G 1996 *J. Appl. Phys.* **79** 8856
- [29] Liao W S and Lee S C 1996 *J. Appl. Phys.* **80** 1171
- [30] Boyd I W and Wilson J I B 1982 *J. Appl. Phys.* **543** 4166
- [31] Nakamura M, Mochizuki Y, Usami K, Itoh Y and Nozaki T 1984 *Solid State Com.* **50** 1079
- [32] Pai P G, Chao S S, Takagi Y and Lucovsky G 1986 *J. Vacuum Sci. Technol. A* **4** 689
- [33] Pliskin W A and Lehman H S 1965 *Journal of the Electrochemical Society* **112** 1013
- [34] Luft W and Tsuo Y S New York 1993 *Hydrogenated Amorphous Silicon Alloy Deposition Processes*

Figures captions

Table1. Different possible peak assignments.

Figure 1. Schematic top view of the experimental arrangement, showing the plasma reactor, the FTIR measurement, the mass spectrometer measurement and the He-Ne laser scattering diagnostic.

Figure 2. Infrared transmitted spectra through the gas (subscript 1) and through the plasma, under steady state conditions (superscript 2), for two different argon/silane/oxygen gas mixture. a) 35.3 sccm of argon + 17 sccm of silane + 7.7 sccm of oxygen b) 49.2 sccm of argon + 3.1 sccm of silane + 7.7 sccm of oxygen. Plasma parameters: pressure at 0.2 mbar, rf plasma power 10 W at 13.56 MHz. The reactor is at room temperature.

Figure 3. The absorbance spectra, under steady state conditions, of particles created in two different gas mixtures a) 35.3 sccm of argon + 17 sccm of silane + 7.7 sccm of oxygen and b) 49.2 sccm of argon + 3.1 sccm of silane + 7.7 sccm of oxygen. c) the FTIR absorbance spectrum of SiO₂ "Ludox LS" colloidal powder. Same plasma parameters as for figure 2.

Figure 4. The absorbance spectra of silicon powder formed in argon (48 sccm) / silane (2 sccm) plasma and trapped in discharge of a) 48 sccm of argon, and b) of 48 sccm of argon and 7.7 sccm of oxygen. Same plasma parameters as for figure 2.

Figure 5. The Balzers mass spectrometry measurements, under steady state conditions, for modulated plasma with a time (plasma on) of 110 μ s and a pause (plasma off) of 300 μ s. These raw data, acquired with low mass resolution, are uncorrected for any mass-dependent fall-off in sensitivity. a) b) and c) represent the negative ions, the positive ions and the neutrals in pure silane plasma respectively. d), e) and f) represent the negative ions, the positive ions and the

neutrals in diluted silane / oxygen (10% in volume) plasma respectively. Plasma parameters: pressure at 0.1 mbar at 13.56 MHz. The ground electrode was heated to 200 °C.

Figure 6. The negative ion mass spectra at high resolution in a pure silane plasma in a range of 20 to 100 amu for a) and in a range of 365 to 455 amu for c). b) and d) represents the negative ions in diluted silane / oxygen (10% in volume) plasma in the same mass range as a) and c) respectively. Same plasma parameters as for figure 5.

Figure 7. A comparison of the positive ion mass spectra in silane / oxygen (10% in volume) plasma obtained from a) the modelling and b) the experimental measurements.

Peak	Wavenumber (cm ⁻¹)	Mode Assignments	References
A	630-720	SiH bending, rocking, wagging SiH ₂ , SiH ₃ rocking (SiH ₂) _n shear and rocking	[20-28]
B	730-830	730 cm ⁻¹ rocking and 830 cm ⁻¹ bending mode of O ₂ Si-H ₂ 780 cm ⁻¹ is a Si-H (bending motion perpendicular to Si-H bond)+ Si-O-Si (bending + small stretching). O-Si-H cis-configuration. O and H bonded to common Si- site 800 cm ⁻¹ : O-Si-O bending 814 cm ⁻¹ : Si-O-Si bending of a thermal SiO ₂ layer	[29] [23,24]
C	835 and 843	-(SiH ₂) _n wagging; =(SiH ₂) _n wagging; Triple-SiH rocking	[30] [4] [27]
D	850 and 890 875	Si-H bending in SiH ₂ and SiH ₃ (SiH ₂) _n wagging and scissors + peak at 2090 cm ⁻¹ : SiH ₂ isolated stretching Peak arise from structural combination of Si-(O ₂ Si ₂), Si-(O ₃ Si) and Si-(O ₄)	[20, 21, 28] [26] [23] [31]
E	920-1085	Relation Ship between IR absorption peak position and the stoichiometry of SiO _x (x=2 at 1085 cm ⁻¹) 940 cm ⁻¹ : isolated Si-O-Si stretching and 980 cm ⁻¹ : oxygen asymmetric stretching of Si-O-Si in <i>cis</i> and <i>trans</i> configuration and 1030 cm ⁻¹ : Si-O-Si Stretching mode in which the silicon atoms are bonded to other oxygen atom 1042+870+800 cm ⁻¹ : Si ₂ O ₃ layer feature (intermediate between SiO and SiO ₂)	[31,32] [23,24]
F	1150	SiO surface mode	[34]
G	1230	Longitudinal Optical (LO) phonon mode of SiO ₂ only active for platelet particles smaller than $\lambda/2\pi n$	[15]

Table I

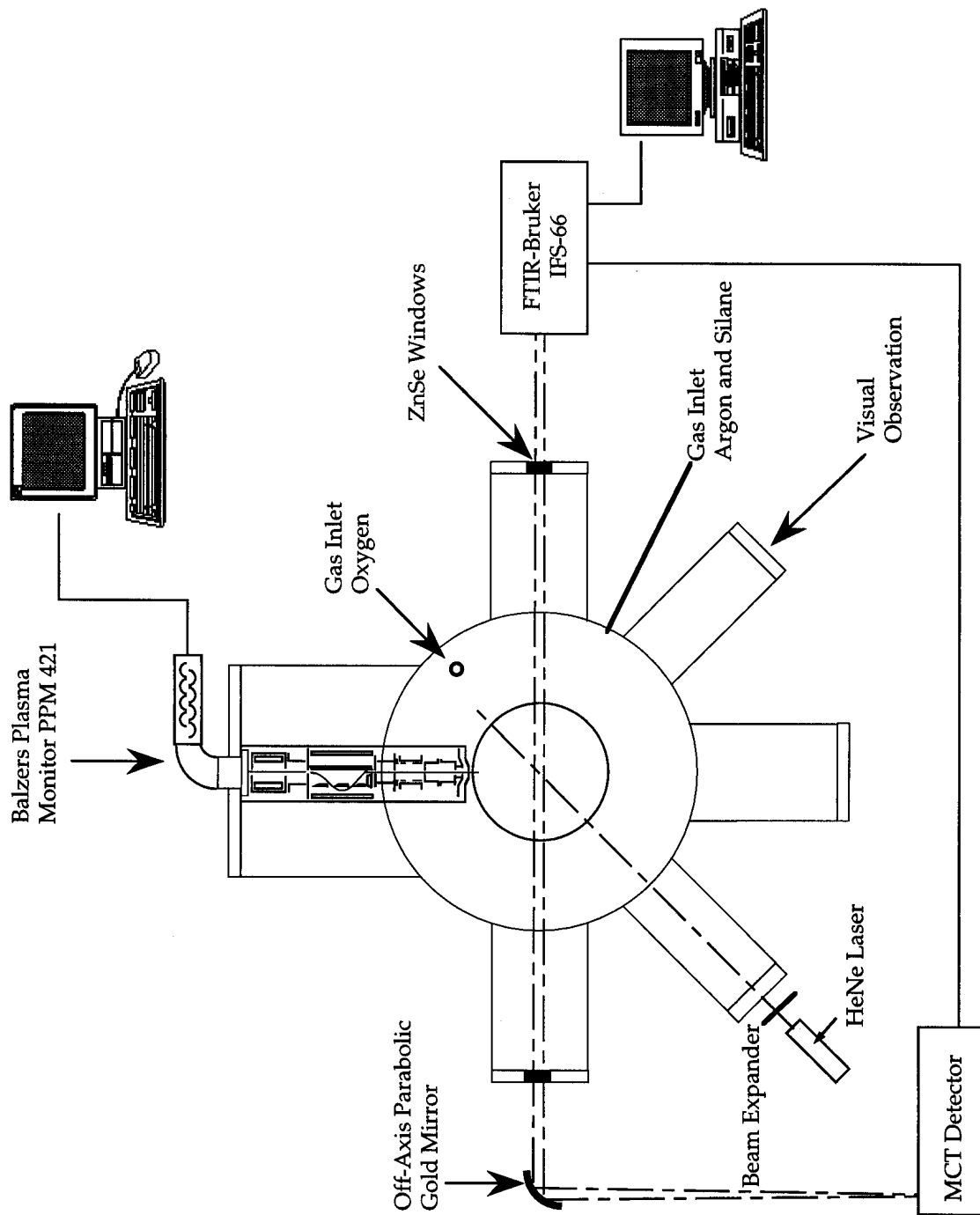


Fig. 1

11

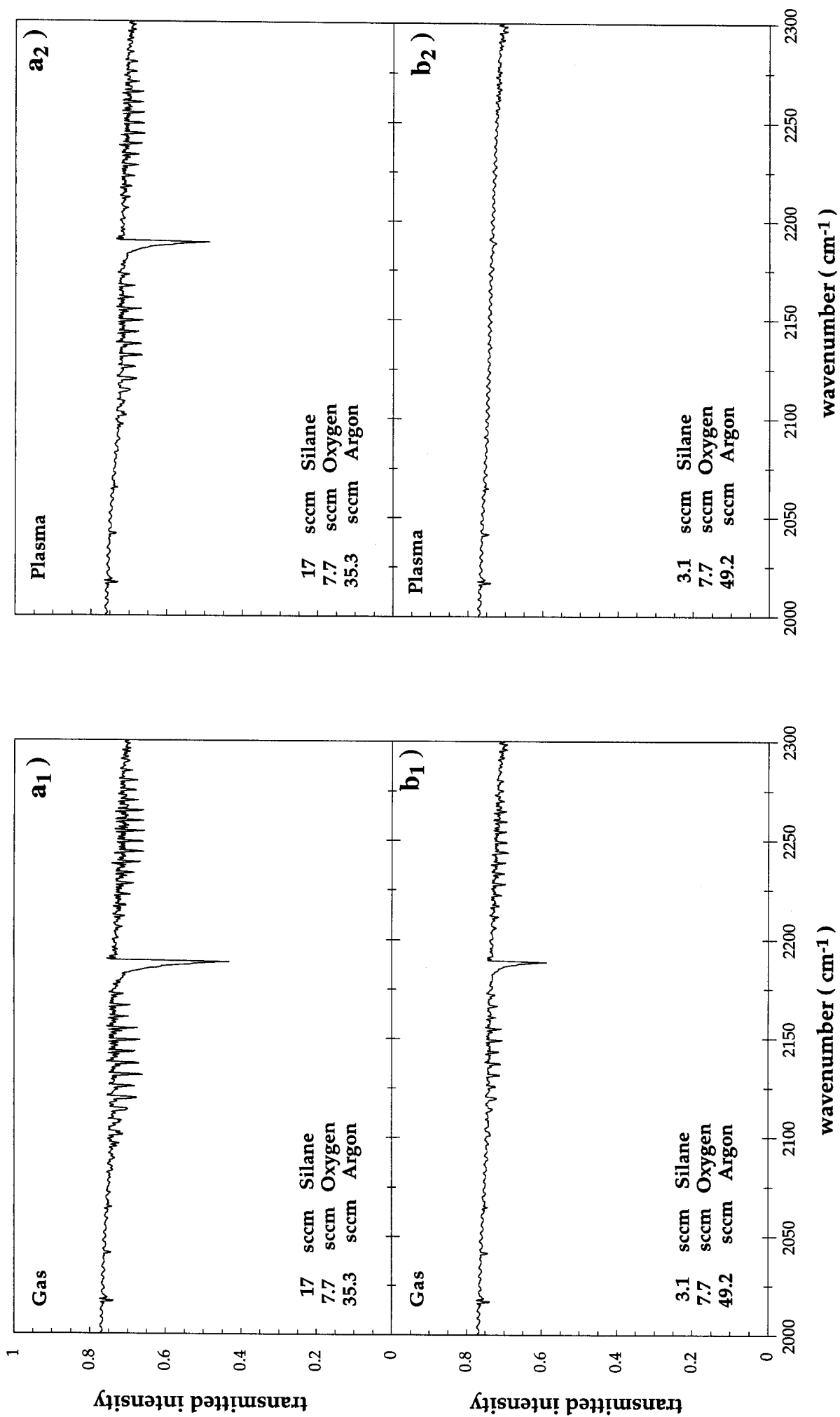


Fig. 2

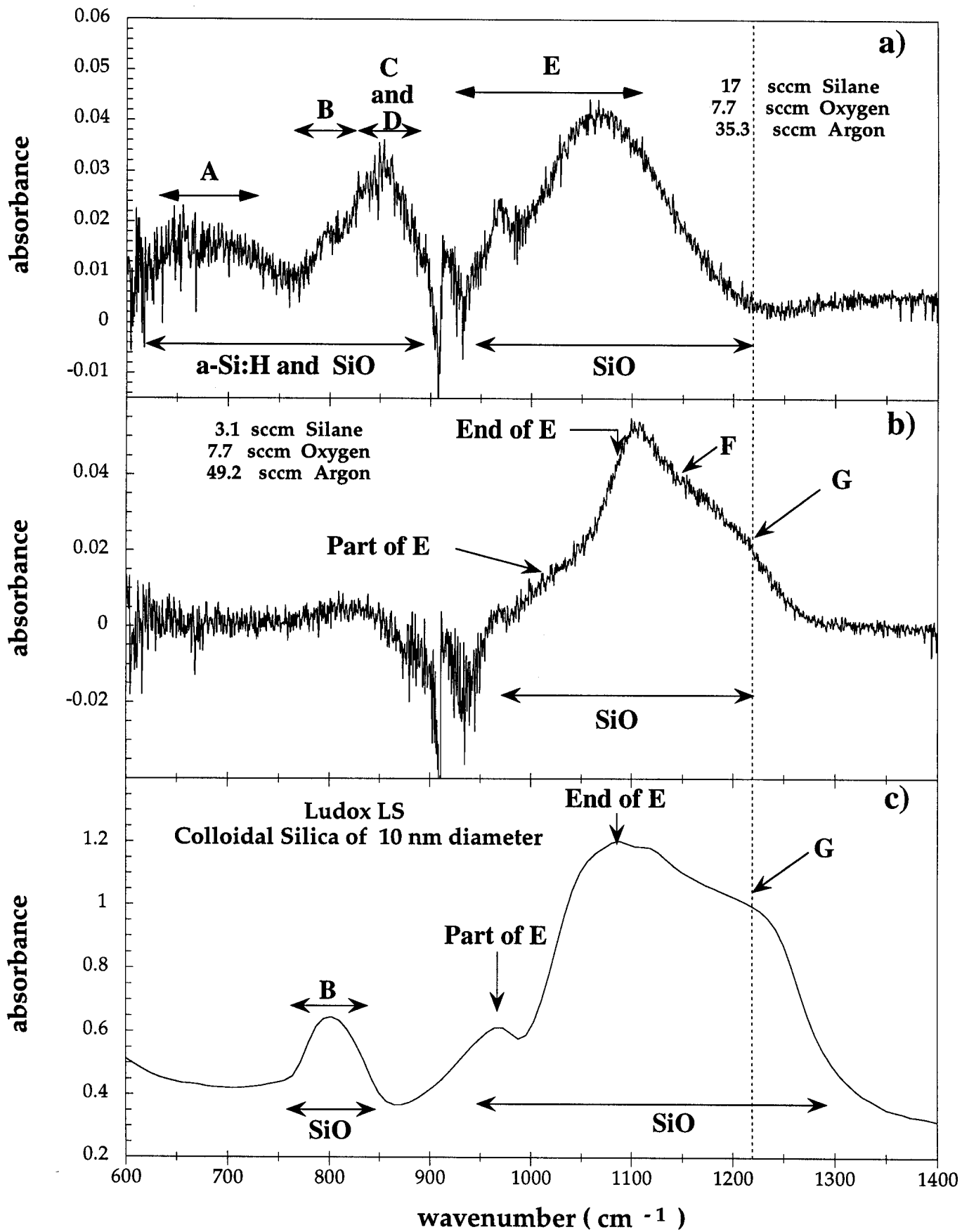


Fig. 3

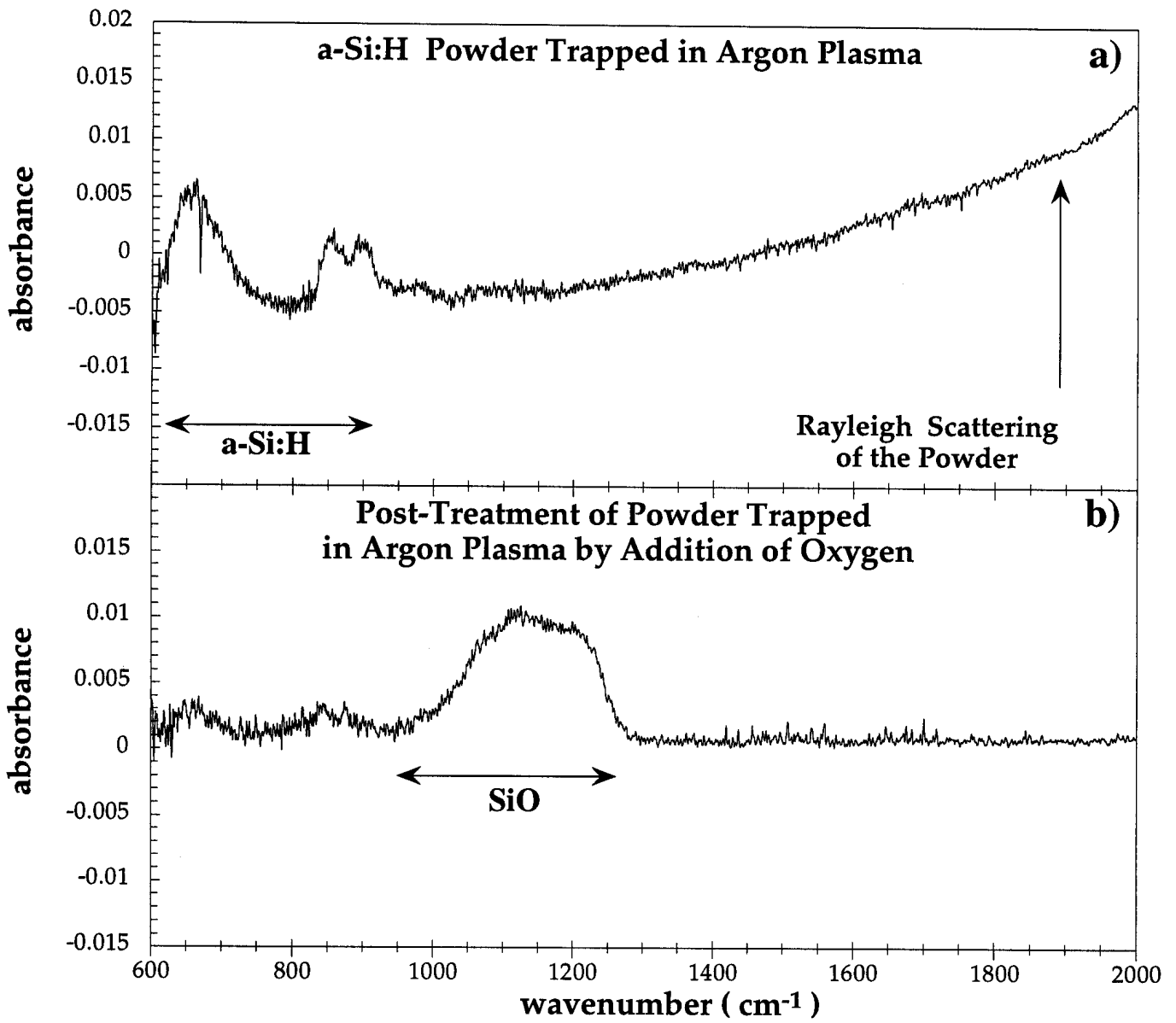


Fig. 4

71

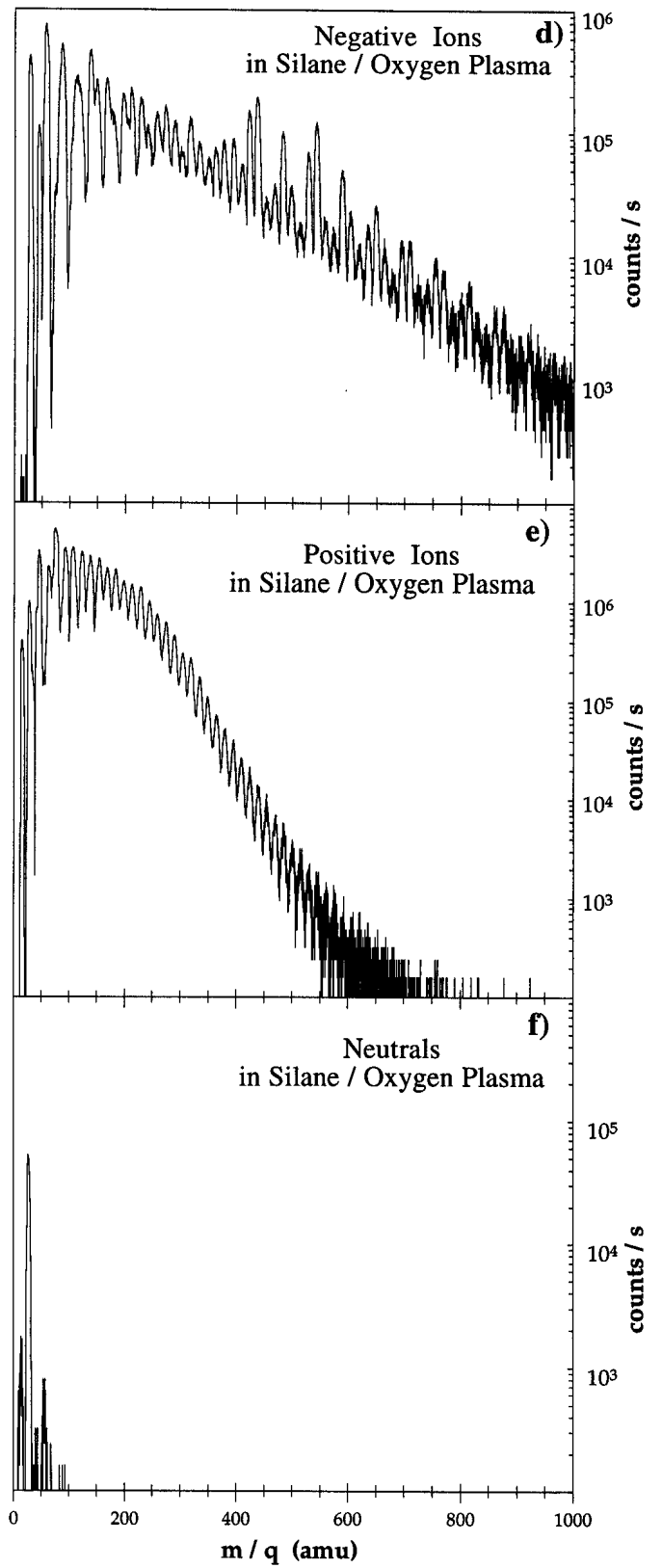
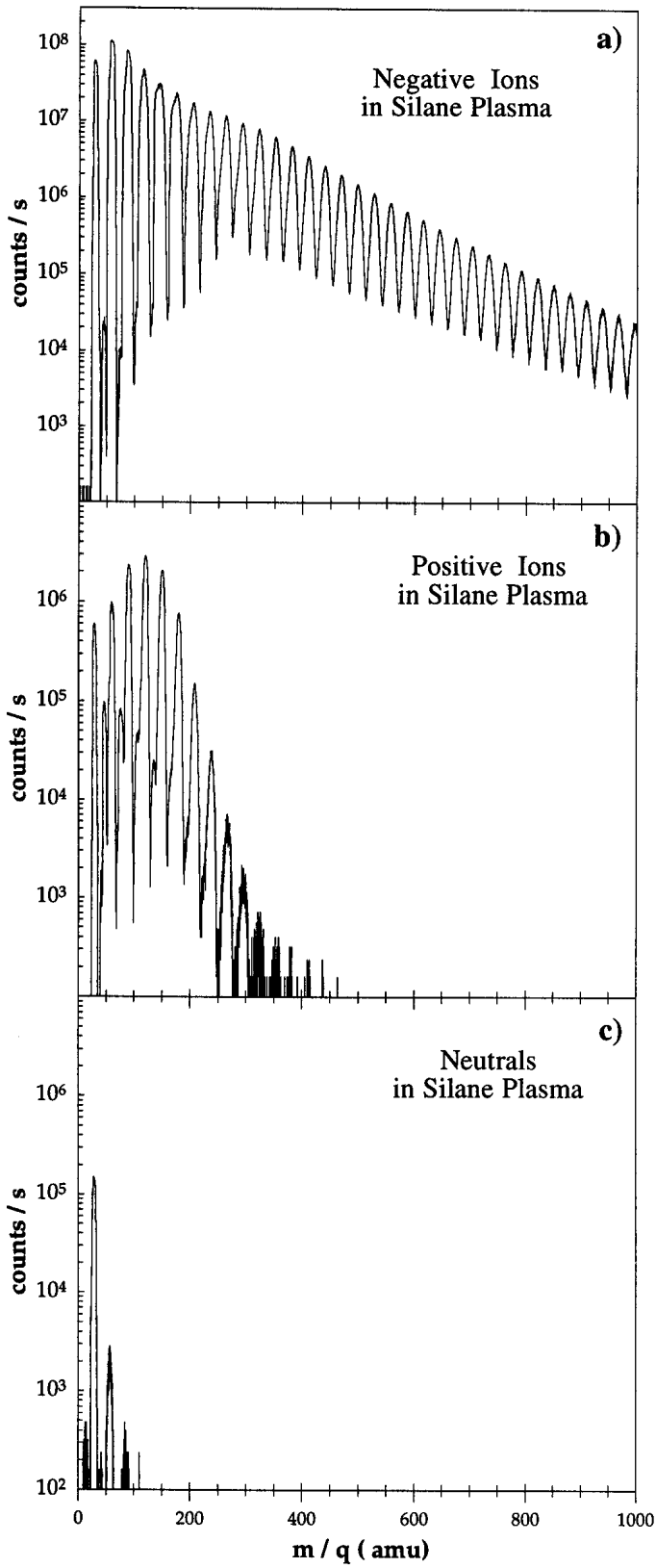


Fig. 5

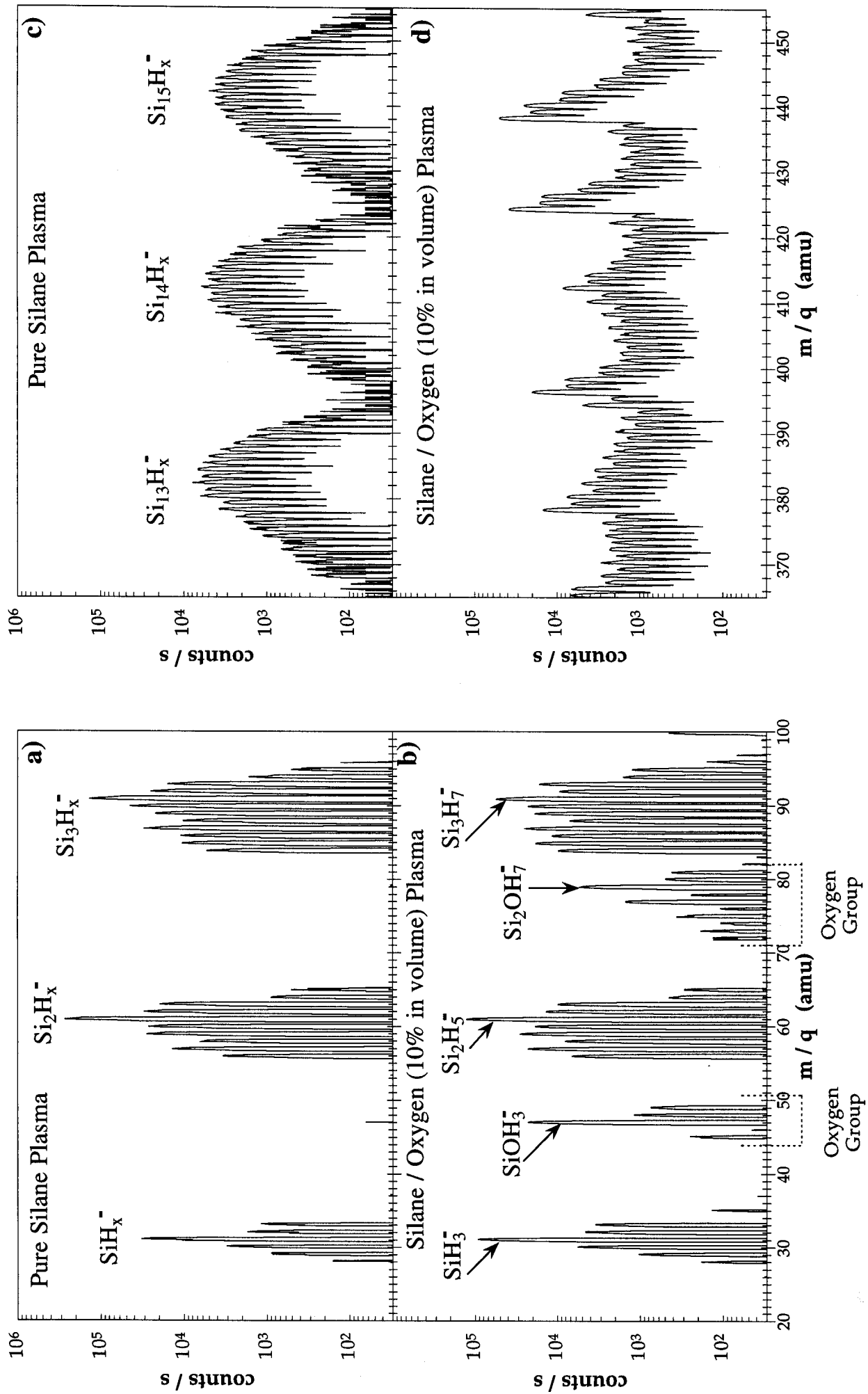


Fig. 6

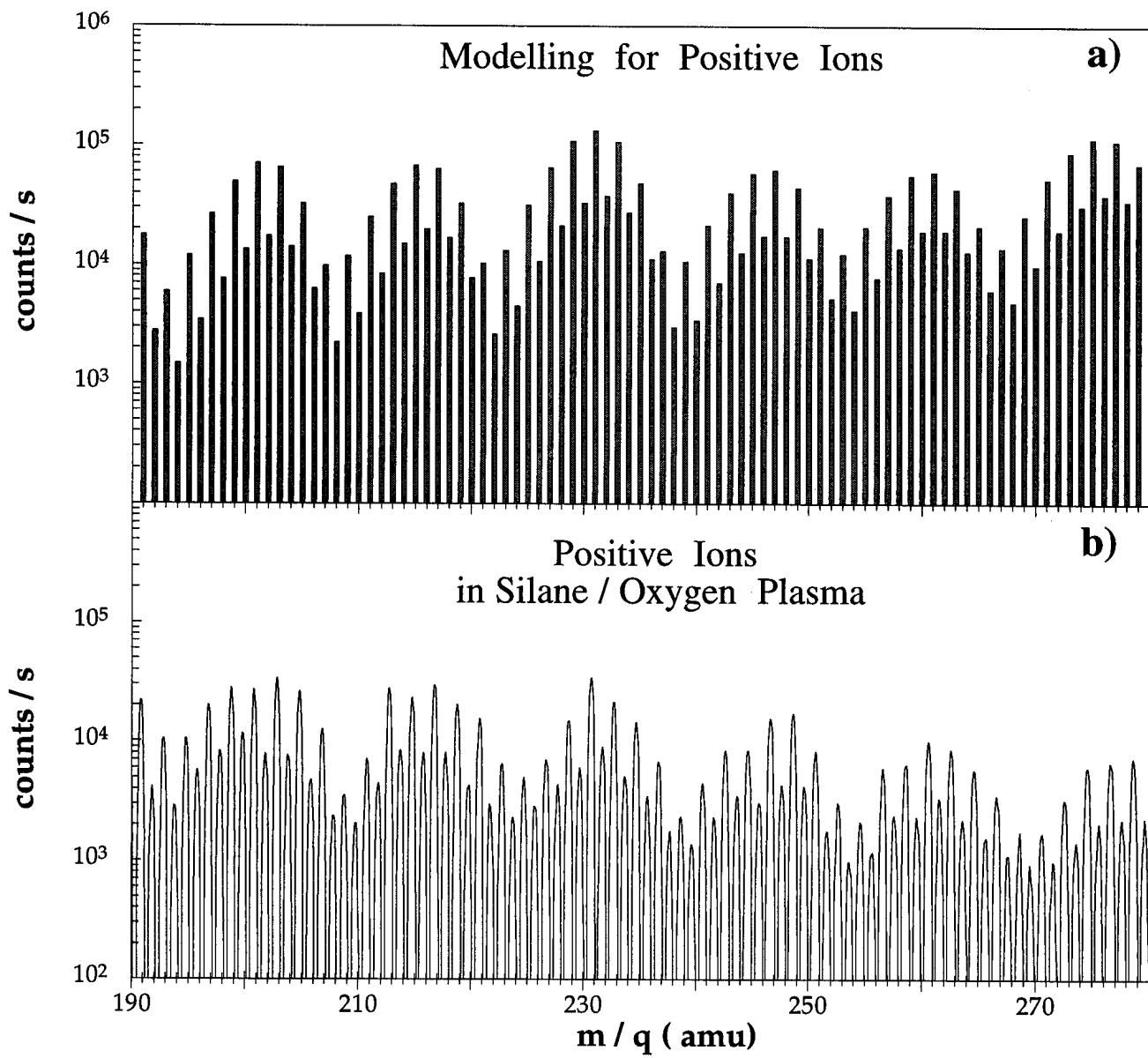


Fig. 7